

Articles

Synthesis and Characterization of Triosmium Clusters Containing the Bidentate Ligand $\text{Ph}_2\text{PCH}_2\text{CH}_2\text{SMe}$: Detection of an Isomerization Reaction Involving Bridging and Chelating Ligand Coordination Modes

Roger Persson,[†] Magda Monari,[‡] Roberto Gobetto,[§] Andrea Russo,[§] Silvio Aime,[§] Maria José Calhorda,^{||} and Ebbe Nordlander^{*,†}

Inorganic Chemistry 1, Chemical Center, Lund University, Box 124, SE-221 00 Lund, Sweden, Dipartimento di Chimica 'G. Ciamician', Università degli Studi di Bologna, Via Selmi 2, Bologna 40126, Italy, Dipartimento di Chimica Inorganica, Chimica Fisica e Chimica dei Materiali, Università di Torino, Via P. Giuria 7, 10125 Torino, Italy, and ITQB, Av. República, EAN, 2781-901 Oeiras and Departamento de Química e Bioquímica, Faculdade de Ciências, Universidade de Lisboa, Campo Grande, 1749-016 Lisboa, Portugal

Received March 21, 2001

Diphenylphosphinoethylene methyl sulfide, $\text{Ph}_2\text{PCH}_2\text{CH}_2\text{SMe}$, reacts with $[\text{Os}_3(\text{CO})_{11}(\text{NCMe})]$ yielding $[\text{Os}_3(\text{CO})_{11}(\text{Ph}_2\text{PCH}_2\text{CH}_2\text{SMe})]$. Treatment of $[\text{Os}_3(\text{CO})_{10}(\text{NCMe})_2]$ with 1 equiv of the P,S ligand initially yields the cluster 1,2- $[\text{Os}_3(\text{CO})_{10}(\mu\text{-Ph}_2\text{PCH}_2\text{CH}_2\text{SMe})]$, in which the phosphine and the thioether moieties coordinate to different metal atoms of the metal triangle; addition of two or more equivalents of the ligand yields 1,2- $[\text{Os}_3(\text{CO})_{10}(\mu\text{-Ph}_2\text{PCH}_2\text{CH}_2\text{SMe})]$ and $[\text{Os}_3(\text{CO})_{10}(\text{Ph}_2\text{PCH}_2\text{CH}_2\text{SMe})_2]$. The cluster 1,2- $[\text{Os}_3(\text{CO})_{10}(\mu\text{-Ph}_2\text{PCH}_2\text{CH}_2\text{SMe})]$ is metastable and undergoes a slow isomerization reaction at room temperature to form 1,1- $[\text{Os}_3(\text{CO})_{10}(\text{Ph}_2\text{PCH}_2\text{CH}_2\text{SMe})]$, in which the ligand chelates one Os atom. Computational modeling of 1,2- and 1,1- $[\text{Os}_3(\text{CO})_{10}(\text{Ph}_2\text{PCH}_2\text{CH}_2\text{SMe})]$ indicates that the two clusters are of similar stability, with the latter isomer being of slightly lower energy. The dynamic behavior of the clusters have been investigated by variable-temperature $^{13}\text{C}\{^1\text{H}\}$ and $^{31}\text{P}\{^1\text{H}\}$ NMR, and the kinetics of the isomerization reaction have been measured. The latter indicate that the isomerization proceeds via an associative mechanism which is proposed to involve an intramolecular nucleophilic attack by the coordinated sulfur on an osmium atom. The solid state structures of $[\text{Os}_3(\text{CO})_{11}(\text{Ph}_2\text{PCH}_2\text{CH}_2\text{SMe})]$, 1,2- $[\text{Os}_3(\text{CO})_{10}(\mu\text{-Ph}_2\text{PCH}_2\text{CH}_2\text{SMe})]$, and 1,1- $[\text{Os}_3(\text{CO})_{10}(\text{Ph}_2\text{PCH}_2\text{CH}_2\text{SMe})]$ are reported.

Introduction

The chemistry of asymmetric bidentate ligands is receiving considerable attention and a number of transition metal complexes containing bi- or polydentate phosphine-based ligands, e.g., phosphine-amine (P,N),¹ phosphine-ether (P,O),² and phosphine-thiolate or phos-

phine-thioether (P,S)³ ligands, have been reported in recent years. Many such metal complexes act as modest to good catalysts in different asymmetric transformations, e.g., allylic alkylations, hydrogenations, and Heck reactions.^{1–3} The coordination chemistry of phosphine-ether and phosphine-thioether ligands, including chiral ligands, has been studied by several investigators.^{3b,4–6} For example, it has been found that the phosphine $\text{iPr}_2\text{PCH}_2\text{CH}_2\text{OMe}$ may coordinate in unidentate (through the phosphorus atom) and bidentate coordination modes in Ru(II) complexes; examples include $[\text{RuCl}_2(\text{CO})_2(\eta^1\text{-}\text{iPr}_2\text{PCH}_2\text{CH}_2\text{OMe})_2]$,⁵ $[\text{RuCl}_2(\eta^2\text{-}\text{iPr}_2\text{PCH}_2\text{CH}_2\text{OMe})_2]$,⁵

* Corresponding author. Fax: +46 46 222 4439. E-mail: Ebbe.Nordlander@inorg.lu.se.

† Lund University.

‡ Università degli Studi di Bologna.

§ Università di Torino.

|| Universidade de Lisboa.

(1) (a) Selvakumar, K.; Valentini, M.; Wörle, M. W.; Pregosin, P. S.; Albinati, A. *Organometallics* **1999**, *18*, 1207. (b) Wehman, P.; van Donge, H. M. A.; Hagos, A.; Kamer, P. C.; van Leeuwen, P. W. N. M. *J. Organomet. Chem.* **1997**, *529*, 387. (c) Nagel, U.; Nedden, H. G. *Chem. Ber./Recl. Trav. Chim. Pays-Bas*, **1997**, *130*, 535. (d) Kubota, H.; Koga, K. *Heterocycles* **1996**, *42*, 543.

(2) (a) Kadyrov, R.; Heinicke, J.; Kindermann, M. K.; Heller, D.; Fischer, C.; Selke, R.; Fischer, A. K.; Jones, P. G. *Chem. Ber./Recl. Trav. Chim. Pays-Bas*, **1997**, *130*, 1663. (b) Heinicke, J.; Jux, U.; Kadyrov, R.; He, M. *Heteroatom. Chem.* **1997**, *8*, 383. (c) Werner, H.; Stark, A.; Schultz, M. Wolf, J. *Organometallics* **1992**, *11*, 1126. (d) Steinert, P.; Werner, H. *Organometallics* **1994**, *13*, 2677.

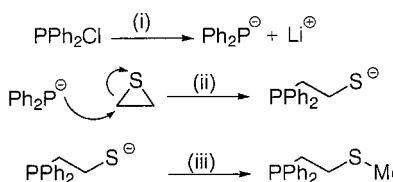
(3) (a) Selvakumar, K.; Valentini, M.; Pregosin, P. S.; Albinati, A. *Organometallics* **1999**, *18*, 4591. (b) Hauptman, E.; Fagan, P. J.; Marshall, W. *Organometallics* **1999**, *18*, 2061, and references therein.

(4) (a) Degischer, G.; Schwarzenbach, G. *Helv. Chim. Acta* **1966**, *49*, 1927. (b) Schwarzenbach, G. *Chem. Zvesti* **1965**, *19*, 200. (b) Persson, R.; Carrano, C. J.; Nordlander, E. *6th Platinum Metals Conference*; York, U.K., 1996; p 133.

(5) Wolfsberger, W.; Burkart, W.; Werner, H. *Z. Naturforsch.* **1995**, *50b*, 168.

(6) Lindner, E.; Andres, B. *Chem. Ber.* **1987**, *120*, 761.

Scheme 1. Schematic Depiction of the Synthetic Route to $\text{PPh}_2\text{CH}_2\text{CH}_2\text{SMe}^a$



^a (i) Li, thf, room temperature (rt), 20 h; (ii) thf, -40 °C; (iii) 1 equiv iodomethane, thf, rt.

and $[\text{RuCl}_2(\eta^2\text{-Ph}_2\text{PCH}_2\text{CH}_2\text{OMe})_2]$.⁶ Mononuclear transition metal (e.g., Mo, Rh, Ir) complexes containing the related P,S ligand $\text{Ph}_2\text{PCH}_2\text{CH}_2\text{SMe}$ have also been reported.⁷

Less attention has been paid to the study of mixed donor ligands coordinated to electron-rich polynuclear transition metal complexes. We are presently studying possible coordination modes of P,S and P,S,P (phosphine-thiolate or phosphine-thioether) ligands to tri-nuclear osmium and ruthenium clusters in low oxidation states. Here we report the preparation and interconversion of derivatives of $[\text{Os}_3(\text{CO})_{12}]$ containing $\text{Ph}_2\text{PCH}_2\text{CH}_2\text{SMe}$ as well as nonrigid effects attributed to coordination of the P,S ligand to the triosmium cluster.

Results and Discussion

The original synthesis of $\text{Ph}_2\text{PCH}_2\text{CH}_2\text{SMe}$ involves P-C bond formation via nucleophilic attack of lithium diphenylphosphide⁸ or by Ph_2PMgBr ⁹ on 2-chloroethyl methyl sulfide. An outline of our synthetic route to this ligand—which is similar to the method recently employed for the synthesis of chiral P,S ligands¹⁰—is shown in Scheme 1. Lithium diphenyl phosphide is generated by reacting PPh_2Cl with lithium in tetrahydrofuran.¹¹ The nucleophilic ring opening of thiirane by diphenyl phosphide, followed by reaction with iodomethane, affords $\text{Ph}_2\text{PCH}_2\text{CH}_2\text{SMe}$ in good yield. Purification of the crude product by column chromatography gives the ligand as a white crystalline solid in ca. 40% yield. The product was characterized by ¹H and ³¹P NMR and elemental analysis (cf. Experimental Section).

Synthesis and Characterization of $[\text{Os}_3(\text{CO})_{11}(\text{Ph}_2\text{PCH}_2\text{CH}_2\text{SCH}_3)]$ (1). Reaction of a stoichiometric amount of $\text{Ph}_2\text{PCH}_2\text{CH}_2\text{SMe}$ with $[\text{Os}_3(\text{CO})_{11}(\text{NCMe})]$ at ambient temperature leads to formation of $[\text{Os}_3(\text{CO})_{11}(\text{Ph}_2\text{PCH}_2\text{CH}_2\text{SCH}_3)]$, **1**, exclusively. Comparison of the $\nu_{\text{C}-\text{O}}$ IR stretching frequency pattern of **1** to known clusters¹² indicates that the cluster contains one phosphine group coordinated in an equatorial position and a peak at $m/z = 1140$ in the FAB mass spectrum matches the calculated molecular mass. The ¹H NMR spectrum of **1** reveals that the resonance assigned to

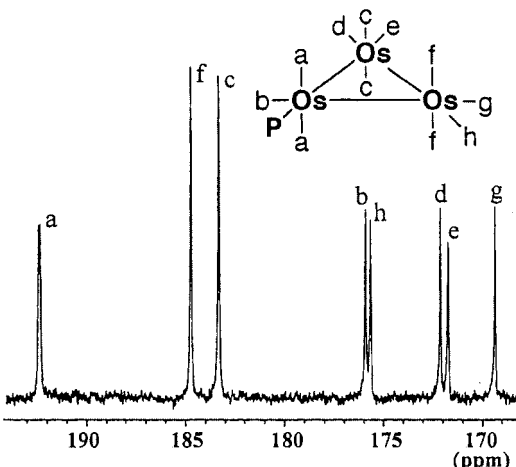


Figure 1. Limiting ¹³C{¹H} NMR spectrum of $[\text{Os}_3(\text{CO})_{11}(\text{Ph}_2\text{PCH}_2\text{CH}_2\text{SMe})]$, **1**, recorded at -60 °C (carbonyl region) and assignment of the carbonyl resonances. The P,S ligand is denoted by the letter "P".

the methylene protons next to the phosphorus of the P,S ligand is shifted downfield by ca. 0.3 ppm upon coordination to the cluster. In the low-temperature (213 K) limited ¹³C{¹H} NMR spectrum of **2**, eight resonances with the intensity ratios 2:2:2:1:1:1:1:1 were observed (Figure 1). The three low-field resonances at $\delta > 185$ ppm are assigned to six axial carbonyls, and the remaining resonances at $\delta > 160$ ppm are assigned to carbonyls in equatorial positions. For the resonance at 192.3 ppm (resonance *a* in Figure 1), a $^2J(^{13}\text{C}-^{31}\text{P})$ coupling of 9.1 Hz was observed. These observations are consistent with a cluster unit consisting of 11 linear carbonyl ligands—five equatorial and six axial—and the assignment of the resonances is similar to those for $[\text{Os}_3(\text{CO})_{11}(\text{PR}_3)]$ (R = Et,¹³OMe¹⁴). One singlet was detected at $\delta = -11.17$ ppm in the ³¹P{¹H} NMR spectrum of $[\text{Os}_3(\text{CO})_{11}(\text{Ph}_2\text{PCH}_2\text{CH}_2\text{SMe})]$, which is similar to previously reported ³¹P chemical shifts for $[\text{Os}_3(\text{CO})_{11}(\text{phosphine})]$ clusters.^{15,16}

Crystal and Molecular Structure of **1.** To confirm the structure of **1**, its crystal structure was determined by X-ray diffraction. The molecular structure of $[\text{Os}_3(\text{CO})_{11}(\text{Ph}_2\text{PCH}_2\text{CH}_2\text{SCH}_3)]$, **1**, is depicted in Figure 2, and selected bond lengths and angles are listed in Table 1. The molecule consists of an isosceles triangle of Os atoms with 11 terminal carbonyls and the phosphorus atom of the P,S ligand occupying an equatorial coordination site. The Os—P distance [2.325(3) Å] falls in the range 2.285–2.399 Å, which is typical for this class of compounds.¹⁷ The Os—Os bonds are slightly shorter than the average metal–metal distance of 2.877(3) Å

(13) Johnson, B. F. G.; Reichert, B. E.; Schorpp, K. T. *J. Chem. Soc., Dalton Trans.* **1976**, 1403.

(14) Alex, R. F.; Pomeroy, R. K. *Organometallics* **1987**, 6, 2437.

(15) (a) Cartwright, S.; Clucas, J. A.; Dawson, R. H.; Foster, D. F.; Harding, M. M.; Smith, A. K. *J. Organomet. Chem.* **1986**, 302, 403. (b) Clucas, J. A.; Foster, D. F.; Harding, M. M.; Smith, A. K. *J. Chem. Soc., Chem. Commun.* **1984**, 949. (c) Foster, D. F.; Harrison, J.; Nicholls, B. S.; Smith, A. K. *J. Organomet. Chem.* **1985**, 295, 99. (d) Clucas, J. A.; Harding, M. M.; Smith, A. K. *J. Chem. Soc., Chem. Commun.* **1985**, 1280. (e) Deeming, A. J.; Donovan-Mtunzi, S.; Kabir, S. E. *J. Organomet. Chem.* **1984**, 276, C65. (f) Deeming, A. J.; Hardcastle, K. I.; Kabir, S. E. *J. Chem. Soc., Dalton Trans.* **1988**, 827. (g) Deeming, A. J.; Kabir, S. E. *J. Organomet. Chem.* **1988**, 340, 359.

(16) Churchill, M. R.; DeBoer, B. G. *Inorg. Chem.* **1977**, 16, 878.

(17) Bruce, M. I.; Lidell, M. J.; Hughes, C. A.; Patrick, J. M.; Skelton, B. W.; White, A. H., *J. Organomet. Chem.* **1988**, 347, 181.

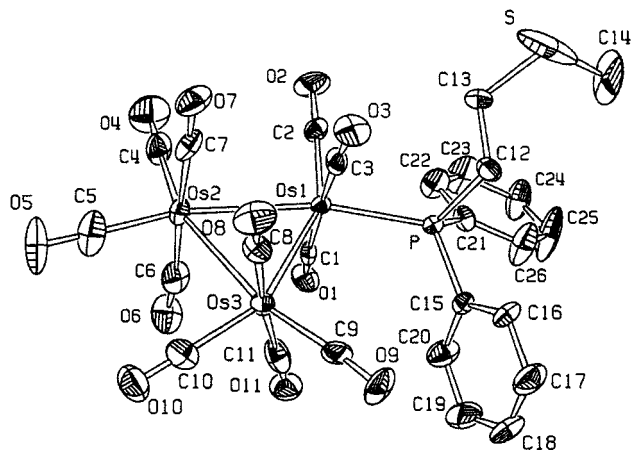


Figure 2. ORTEP drawing of $[\text{Os}_3(\text{CO})_{11}(\text{Ph}_2\text{PCH}_2\text{CH}_2\text{SMe})]$, **1**. Thermal ellipsoids are drawn at the 30% level. Hydrogen atoms have been omitted for clarity.

Table 1. Selected Bond Lengths (Å) and Angles (deg) for $[\text{Os}_3(\text{CO})_{11}(\text{Ph}_2\text{PCH}_2\text{CH}_2\text{SMe})]$ (2)

Os(1)–Os(2)	2.849(1)	Os(2)–C(7)	1.93(1)
Os(2)–Os(3)	2.871(1)	Os(3)–C(8)	1.92(1)
Os(1)–Os(3)	2.849(1)	Os(3)–C(9)	1.91(1)
Os(1)–P	2.325(3)	Os(3)–C(10)	1.88(1)
C(13)–S	1.78(1)	Os(3)–C(11)	1.96(1)
C(14)–S	1.80(2)	C(1)–O(1)	1.15(1)
P–C(12)	1.84(1)	C(2)–O(2)	1.13(1)
P–C(15)	1.82(1)	C(3)–O(3)	1.15(1)
P–C(21)	1.78(1)	C(4)–O(4)	1.14(1)
C(12)–C(13)	1.52(2)	C(5)–O(5)	1.13(1)
Os(1)–C(2)	1.87(1)	C(6)–O(6)	1.14(1)
Os(1)–C(3)	1.94(1)	C(7)–O(7)	1.14(1)
Os(1)–C(1)	1.91(1)	C(8)–O(8)	1.14(1)
Os(2)–C(4)	1.88(1)	C(9)–O(9)	1.14(1)
Os(2)–C(5)	1.88(1)	C(10)–O(10)	1.12(1)
Os(2)–C(6)	1.95(1)	C(11)–O(11)	1.13(1)
C(1)–Os(1)–C(3)	173.7(5)	C(6)–Os(2)–Os(3)	84.2(4)
C(11)–Os(3)–C(8)	174.3(6)	C(5)–Os(2)–C(4)	99.1(7)
C(6)–Os(2)–C(7)	175.9(6)	Os(1)–P–C(12)	115.2(3)
C(2)–Os(1)–P	100.5(4)	Os(1)–P–C(15)	117.5(3)
C(11)–Os(3)–Os(1)	84.3(4)	C(1)–Os(1)–Os(2)	85.8(3)
C(11)–Os(3)–Os(2)	94.8(4)	C(1)–Os(1)–Os(3)	92.5(4)
P–Os(1)–Os(3)	106.8(1)	C(1)–Os(1)–P	89.7(3)
C(3)–Os(1)–P	88.2(4)	C(7)–Os(2)–C(5)	92.7(7)

found in the parent binary carbonyl $[\text{Os}_3(\text{CO})_{12}]$.¹⁸ The longest Os–Os separation [2.871(1) Å] is that between the osmium atoms not bearing the P,S ligand, which is in contrast to what has been observed in related $[\text{M}_3(\text{CO})_{11}(\text{PR}_3)]$ ($\text{M} = \text{Ru, Os}$) complexes where the M–M distances *cis* to the phosphine ligand are generally the longest and increase with increasing phosphine cone angle.¹⁹ The thioether end of the heterobidentate ligand is oriented with the methyl ligand pointing away from the axial carbonyls. The sulfur atom is not at bonding distance to any osmium atom. The high degree of crowding due to the presence of the bulky phosphine ligand is relieved by twisting of the $\text{Os}(\text{CO})_4$ groups (vide infra).

Synthesis and Characterization of 1,2-[$\text{Os}_3(\text{CO})_{10}(\mu\text{-Ph}_2\text{PCH}_2\text{CH}_2\text{SMe})$] (2). Reaction of $[\text{Os}_3(\text{CO})_{10}(\mu\text{-Ph}_2\text{PCH}_2\text{CH}_2\text{SMe})]$ with 1 equiv of Ph₂PCH₂CH₂SMe

(18) Churchill, M. R.; Lashewycz, K. A.; Shapley, J. R.; Richter, S. I. *Inorg. Chem.* **1980**, *19*, 1277.

(19) (a) Bruce, M. I.; Liddell, M. J.; Hughes, C. A.; Skelton, B. W.; White, A. H. *J. Organomet. Chem.* **1988**, *347*, 157. (b) Bruce, M. I.; Addick, J. M.; Hughes, C. A.; Patrick, J. M.; Skelton, B. W.; White, A. H. *J. Organomet. Chem.* **1988**, *347*, 181. (c) Bruce, M. I.; Liddell, M. J.; Shawkataly, O.; Hughes, C. A.; Skelton, B. W.; White, A. H. *J. Organomet. Chem.* **1988**, *347*, 207.

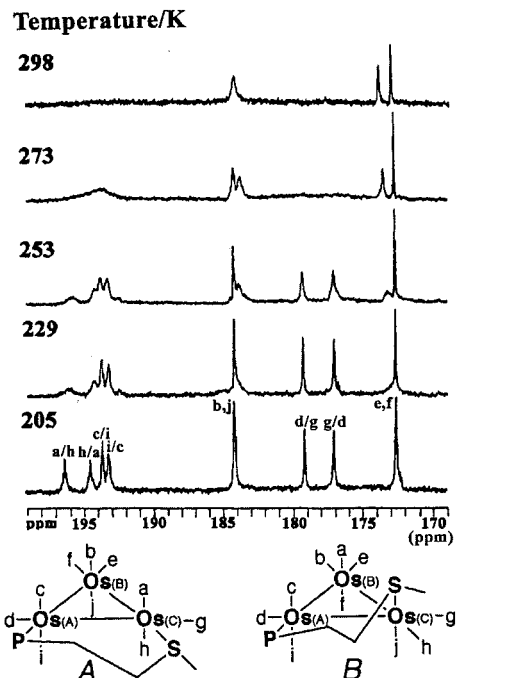


Figure 3. Variable-temperature $^{13}\text{C}\{^1\text{H}\}$ NMR spectra of 1,2-[$\text{Os}_3(\text{CO})_{10}(\mu\text{-Ph}_2\text{PCH}_2\text{CH}_2\text{SMe})$], **2**.

($\text{NCMe})_2$] with 1 equiv of $\text{Ph}_2\text{PCH}_2\text{CH}_2\text{SMe}$ led to the formation of a bright yellow product, which could be identified as 1,2-[$\text{Os}_3(\text{CO})_{10}(\mu\text{-Ph}_2\text{PCH}_2\text{CH}_2\text{SMe})$] (**2**) on the basis of IR, NMR, and mass spectroscopy as well as X-ray diffraction (vide infra). Compound **2** could also be obtained by slow addition of a slight excess of Me_3NO to **1** dissolved in a mixture of CH_2Cl_2 and MeCN . The $\nu_{\text{C–O}}$ stretching pattern of **2** is similar to those of $[\text{Os}_3(\text{CO})_{10}(\mu\text{-}\sigma\text{:}\pi\text{-PPh}_2\text{C}_6\text{H}_4\text{CH}=\text{CH}_2)]^{20}$ and $[\text{Os}_3(\text{CO})_{10}\{\mu\text{-}\sigma\text{:}\pi\text{-CH}_2=\text{CHCH}_2\text{P}(\text{CH}_2\text{CHCH}_2)_2\}]^{21}$, indicating that the ligand spans two osmium atoms and coordinates through its phosphine and thioether moieties. The ^1H NMR spectrum of **2** reveals that the singlet assigned to the methyl group of $\text{Ph}_2\text{PCH}_2\text{CH}_2\text{SMe}$ is shifted downfield by ca. 0.7 ppm upon coordination to the cluster.

The room-temperature ^{13}C NMR spectrum of a ^{13}C -enriched sample of **2** exhibits three resonances at 184.0, 173.7, and 172.8 ppm with the relative ratios 2:1:1 in the carbonyl region. This indicates that, as in the case of **1**, an extensive rearrangement of the carbonyl framework is taking place at room temperature. To get more insight into its fluxional behavior, variable-temperature $^{13}\text{C}\{^1\text{H}\}$ NMR spectra of 1,2-[$\text{Os}_3(\text{CO})_{10}(\mu\text{-Ph}_2\text{PCH}_2\text{CH}_2\text{SMe})$] (**2**) were recorded (Figure 3). The low-temperature limiting spectrum (205 K) reveals the presence of eight resonances at 196.3 ($^2J_{\text{C,C}} = 33.0$ Hz, 1C, *h* or *a*), 194.5 ($^2J_{\text{C,C}} = 33.0$ Hz, 1C, *a* or *h*), 193.5 ($^2J_{\text{C,C}} = 33.4$ Hz, $^2J_{\text{P,C}} = 9.2$ Hz, 1C, *c* or *i*), 193.2 ($^2J_{\text{C,C}} = 33.4$ Hz, $^2J_{\text{P,C}} = 9.2$ Hz, 1C, *i* or *c*), 184.0 (2C, *b* and *j*), 179.0 (1C, *d* or *g*), 176.9 (1C, *g* or *d*), and 172.5 (2C, *e* and *f*, respectively. This is consistent with a C_1 structure with equatorial 1,2-coordination of the P,S ligand (cf. Figure 3, structure **A**). The suggested assignment has been accomplished on the basis of the

(20) Bruce, M. I.; Nicholson, B. K.; Williams, M. L. *J. Organomet. Chem.* **1983**, *243*, 69.

(21) Thapper, A.; Nordlander, E.; King, J. D.; Johnson, B. F. G.; Kane-Maguire, L.; Lewis, J.; Sparr, E.; Raithby, P. Unpublished results.

following considerations: (i) axial carbonyls usually resonate at lower field than equatorial ones; (ii) the occurrence of relatively large values for the $^2J_{\text{C},\text{C}}$ coupling constants within two sets of related axial carbonyls (*c* and *i*; *a* and *h*); (iii) the presence of phosphorus–carbon coupling constants which permit identification of the axial carbonyls bound to the osmium to which the phosphine moiety is coordinated; (iv) the two pairs of resonances (*e* and *f*; *b* and *j* on Os(B)) which should give rise to four separate resonances yield only one signal for the axial and one signal for the equatorial carbonyls because they are too far removed from the ligand. The chemical shifts of **2** are shifted to lower frequencies than **1**; this is probably due to sulfur coordination and parallels the observation that the resonating frequencies decrease as the number of coordinated phosphines increase in a triosmium unit.¹⁴

The highest temperature spectrum (298 K) is consistent with a classical “merry-go-round” process that involves the concerted motion of four axial (*a*, *h*, *c*, and *i*) and two equatorial (*d* and *g*) carbonyls bound to Os(A) and Os(C), respectively (cf. Figure 3). This exchange causes the equivalence of the two axial carbonyls on Os(B) but leaves the equatorial ones (*f*, *e*) on the same atom inequivalent.

The low-temperature process is more intriguing and somewhat puzzling. On going from 205 to 229 K, the main changes are represented by an extensive broadening of resonances *a* and *h*; however, a careful inspection of the spectrum reveals that one of the resonances at 184.0 and one of the carbonyls at 172.5 ppm are involved in an exchange process. This observation is confirmed by the spectrum recorded at 253 K, where there is clear evidence of two broad signals centered at 183.7 and 173.3 ppm, respectively. At this temperature, a slight broadening of the resonance at 184.0 ppm can also be detected. The five resonances (*a*, *b*, *f*, *j*, and *h*) show different line widths, and the observed behavior is tentatively interpreted as an exchange process that averages the main form (*A*, cf. Figure 3) with a minor form (*B*), present in very low concentration, containing the sulfur atom in an axial position. One may envisage a “single-step merry-go-round” process in which the sulfur atom moves from the equatorial position to the axial one (structure *B*) involving the exchange of carbonyls *a*, *b*, *f*, *j*, and *h* according to Figure 3.

The fact that two signals are observed for the axial carbonyls of the osmium atom to which the phosphine moiety is coordinated (*c* and *i*) indicates that the bridging P,S ligand is rigid (on the NMR time scale) at 253 K; that is, there is no “inversion” of its methylene units. The solution structure of **2** is therefore expected to be virtually identical to the solid state structure (vide infra), with the sulfur atom lying slightly out of the triosmium plane, closer to one axial position than the other. The motion of the sulfur is expected to proceed via an associative pathway, without Os–S bond cleavage (vide infra), and it is likely that the sulfur moves to the axial position to which it is closest; motion of the sulfur atom to both of the axial positions of the Os atom bearing the sulfur atom does not take place, otherwise the two resonances *c* and *i* should average into a single signal. The different extent of broadening showed by carbonyls *a*, *b*, *f*, *j*, and *h* is then due to the difference

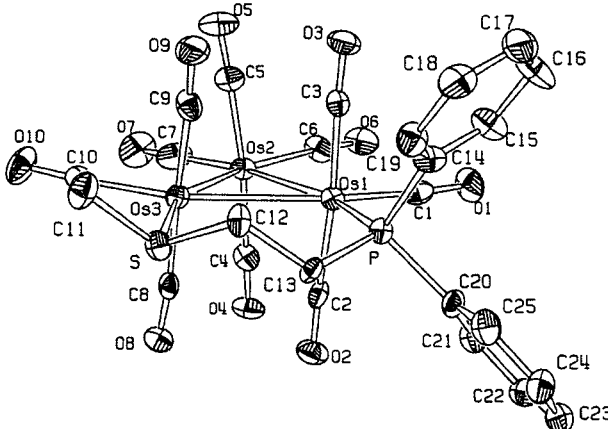


Figure 4. ORTEP diagram of the molecular structure of 1,2-[Os₃(CO)₁₀(μ-Ph₂PCH₂CH₂SMe)], **2**. Thermal ellipsoids are drawn at the 30% level.

in frequency between each of the exchanging pairs in the *A* and *B* forms. Although the chemical shifts of the carbonyls in form *B* are unknown, the observation that carbonyl *j* broadens to a lesser extent than the other ones might be ascribed to the fact that it is exchanging with a carbonyl in the *B* form with a very similar absorption frequency. In fact, on the basis of the observations made for 1,1-[Os₃(CO)₁₀(Ph₂PCH₂CH₂SMe)] (**3**) (vide infra), we expect that the shift of the axial carbonyl *trans* to the sulfur in *B* should be very close to 185 ppm. Structure *B* is a possible key intermediate in the conversion of **2** into 1,1-[Os₃(CO)₁₀(Ph₂PCH₂CH₂SMe)] **3** (vide infra).

The lack of broadening of the resonance labeled *e* in Figure 3 indicates that it is not involved in any dynamic process, which reflects the difference in the phosphorus–osmium and the sulfur–osmium interactions for this compound. The absence of exchange in the *A*–*B* vertical plane can be explained by the phosphine moiety being less inclined to occupy an axial site, possibly due to the steric bulk of its substituents. The effective cone angle of the thioether moiety is less than that of the phosphine, and the sulfur can therefore occupy both sites.

Crystal and Molecular Structure of **2.** Despite its instability in solution, it was possible to obtain crystals of **2** from a CH₂Cl₂/n-hexane solution at 4 °C. The molecular structure of **2** is shown in Figure 4, and relevant bond lengths and angles are reported in Table 2. The phosphino-thioether ligand is coordinated in a bridging mode with the phosphine and the thioether moieties occupying equatorial sites on two different metals. The sulfur, which becomes a chiral center upon coordination, is slightly out of the metal plane [0.339(3) Å]. The Os–P (2.322(3) Å) and the Os–S (2.376(3) Å) separations are similar to those found for triosmium clusters substituted with phosphine and/or thioether ligands.²³ All Os–Os bonds are slightly different in **2**, but the average Os–Os distance is similar to that found in the parent binary carbonyl [Os₃(CO)₁₂] (2.877(3) Å) and in the other clusters reported here. The longest Os–

(22) Adams, R. D. *Organometallics* **1989**, *8*, 1856. (b) Adams, R. D.; Chen, L.; Yamamoto, J. H. *Inorg. Chim. Acta* **1995**, *47*, 229. (c) Adams, R. D.; Pompeo, M. P.; Wu, W.; Yamamoto, J. H. *J. Am. Chem. Soc.* **1993**, *115*, 8207.

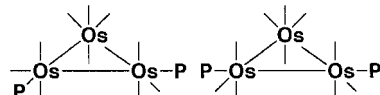
(23) Adams, R. D.; Horvath, I. T.; Segmüller, B. E.; Yang, L. Y. *Organometallics* **1983**, *2*, 144.

Table 2. Selected Bond Lengths (Å) and Angles (deg) for 1,2-[Os₃(CO)₁₀(μ-Ph₂PCH₂CH₂SMe)] (3)

Os(1)–P	2.322(3)	Os(2)–C(4)	1.92(1)
Os(3)–S	2.376(3)	Os(2)–C(5)	1.93(1)
S–C(11)	1.82(1)	Os(2)–C(6)	1.93(1)
S–C(12)	1.80(1)	Os(2)–C(7)	1.93(2)
Os(1)–Os(2)	2.892(2)	Os(3)–C(8)	1.90(1)
Os(2)–Os(3)	2.867(1)	Os(3)–C(9)	1.90(1)
Os(1)–Os(3)	2.911(2)	Os(3)–C(10)	1.88(1)
P–C(13)	1.79(1)	C(1)–O(1)	1.18(2)
P–C(14)	1.82(1)	C(2)–O(2)	1.16(2)
P–C(20)	1.85(1)	C(3)–O(3)	1.19(2)
C(13)–C(12)	1.56(1)	C(4)–O(4)	1.15(2)
Os(1)–C(1)	1.87(1)	C(5)–O(5)	1.15(2)
Os(1)–C(2)	1.93(1)	C(6)–O(6)	1.12(2)
Os(1)–C(3)	1.90(1)	C(7)–O(7)	1.12(2)
C(10)–O(10)	1.15(2)	C(8)–O(8)	1.16(2)
C(9)–O(9)	1.15(2)		
Os(3)–S–C(11)	108.9(5)	C(1)–Os(1)–P	96.9(4)
Os(3)–S–C(12)	110.1(4)	C(8)–Os(3)–Os(2)	83.8(3)
C(9)–Os(3)–S	89.5(4)	C(9)–Os(3)–C(8)	178.1(5)
C(9)–Os(3)–Os(2)	96.1(4)	S–Os(3)–C(10)	97.7(4)
C(3)–Os(3)–P	91.7(4)	S–Os(3)–Os(1)	100.9(1)
C(2)–Os(1)–P	87.7(4)	Os(3)–Os(1)–P	104.2(1)
Os(1)–P–C(13)	113.9(4)	C(9)–Os(3)–Os(1)	85.4(4)
Os(3)–S–C(12)	110.1(4)	C(9)–Os(3)–Os(2)	96.1(4)
P–C(13)–C(12)	118.0(8)	C(5)–Os(2)–Os(3)	81.9(3)
C(11)–S–C(12)	96.3(6)		

Os separation [2.911(2) Å] is the P,S-bridged metal bond, in agreement with the trend observed for the related clusters [Os₃(CO)₁₀(μ-Ph₂P(CH₂)_xPPh₂)] ($x = 2-5$),¹⁵ where the bridged Os–Os bonds are generally slightly longer than the nonbridged ones. The elongation has been suggested to be a consequence of the need to satisfy the conformational requirements of the interconnecting aliphatic chain,¹⁵ but there should also be an electronic origin of this effect, as the two out of phase combinations of lone pairs on the sulfur and the phosphorus require an antibonding combination of Os orbitals and thus contribute to the weakening of the Os–Os bond. The Os–Os bond *trans* to the sulfur in **2** is the shortest [Os(2)–Os(3) 2.867(1) Å], while the metal–metal bond *trans* to the phosphorus is slightly longer. A contraction of the metal–metal bond *trans* to the sulfur (or, in general, *trans* to a strong σ -donor) has been observed in related clusters.^{23,24}

Synthesis and Characterization of [Os₃(CO)₁₀(Ph₂PCH₂CH₂SMe)₂] (3). When [Os₃(CO)₁₀(NCMe)₂] was reacted with 2 equiv of Ph₂PCH₂CH₂SMe, formation of **2** and a red cluster **3** in approximately equal amounts was observed. The red cluster was identified as [Os₃(CO)₁₀{PPh₂(CH₂CH₂SMe)₂} on the basis of IR, NMR, and mass spectroscopy. The ν_{C-O} IR pattern of **3** is consistent with both ligands coordinating through their phosphine moieties only. As was observed for **1** and **2**, the ¹H NMR spectrum of **3** reveals a downfield shift by ca. 0.3 ppm (with respect to the free ligand) for the resonance representing the protons of the methylene unit in α -position to the phosphorus in the P,S ligands. The room-temperature ³¹P{¹H} NMR spectrum of **3** reveals three relatively broad signals (at -16.1, -12.8, and -11.8 ppm) with relative intensity ratios 1:1:2. The resonances at -12.8 and -11.8 ppm merge when increasing the temperature to 40 °C. This is consistent with two interconverting isomers of **3** (Figure 5), as

**Figure 5.** Schematic depiction of the expected isomers of [Os₃(CO)₁₀(Ph₂PCH₂CH₂SMe)₂], **3** (cf. ref 26).

previously observed for [Os₃(CO)₁₀(PR₃)₂] compounds.^{14,25} The formation of both **2** and **3** in the presence of an excess of the P,S ligand indicates that the phosphine moiety of the free ligand and the thioether moiety of the monodentate ligand bind to the cluster at comparable rates. While phosphines are usually considered better nucleophiles than thioethers, the formation of the chelate is thermodynamically favored.

Isomerization of 1,2-[Os₃(CO)₁₀(μ-Ph₂PCH₂CH₂SMe)] (2) into 1,1-[Os₃(CO)₁₀(Ph₂PCH₂CH₂SMe)] (4). Cluster **2** slowly converts into a new cluster (**4**) in solution at room temperature. Cluster **4** could be obtained as an orange-red solid after purification by TLC and recrystallization from CH₂Cl₂/n-hexane. Mass spectrometry and elemental analysis indicated that **4** is a structural isomer of **2**, and NMR and X-ray crystallography (vide infra) showed that **4** is 1,1-[Os₃(CO)₁₀(Ph₂PCH₂CH₂SMe)]. It is known from earlier studies that sulfur undergoes rapid pyramidal inversion when coordinated to transition metal complexes.^{3b,26,27} A broadening effect of the diastereotopic methylene protons next to sulfur due to such an inversion process could be observed in NMR spectra of the complexes [(PCy₂CH₂CH(CH₃)SCH₂C₅(CH₃)₅PdCl₂] and [(PCy₂CH₂CH(CH₃)SCH₂C₅(CH₃)₅NiCl₂] at room temperature.^{3b} However, similar broadening effects of the methylene resonances could not be detected for any of the clusters described here.

Ten resonances were observed in the low-temperature limited (213 K) ¹³C{¹H} NMR spectrum of a sample of **4** that contained approximately 35% ¹³CO (Figure 6). As in the case of **2**, the chemical shifts for **4** are shifted to lower frequencies as compared to **1**. The five low-field resonances at $\delta > 185$ ppm are assigned to axial carbonyls and the remaining resonances to carbonyls in equatorial positions. This assignment is also supported by the presence of two pairs of ²J_{C-C} couplings for the axial carbonyls. The proposed dynamic processes operating in **4** are summarized in Scheme 2. Variable-temperature ¹³C{¹H} NMR spectra (Figure 6) showed that a broadening of four signals (*a*, *h*, *j*, and *b*) assigned to axial and two signals (*c* and *f*) assigned to equatorial carbonyl ligands occurs when the temperature is increased to 240 K. This broadening may be rationalized by a terminal/bridge merry-go-round carbonyl exchange in the vertical plane associated with the metal–metal bond that is bridged by the ligand [Os(A)–Os(B)].¹³ When the temperature is further increased to 265 K, all signals except the resonance at 172.5 ppm are significantly broadened and the low-field signals are almost collapsed. This is consistent with a second exchange process (analogous to that suggested for **2**) operating in the vertical plane of the Os(A)–Os(C) edge.

(25) Leong, W. K.; Liu, Y. *J. Organomet. Chem.* **1999**, *584*, 174.(26) Abel, E. W.; Booth, M.; Orrel, K. G. *J. Chem. Soc., Dalton Trans.* **1980**, 1582.(27) Abel, E. W.; Booth, M.; Orrel, K. G.; Pring, G. M. *J. Chem. Soc., Dalton Trans.* **1981**, 1944.

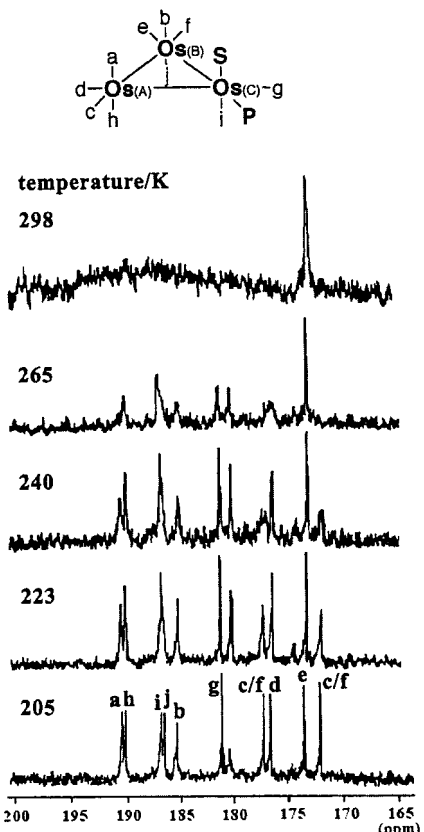
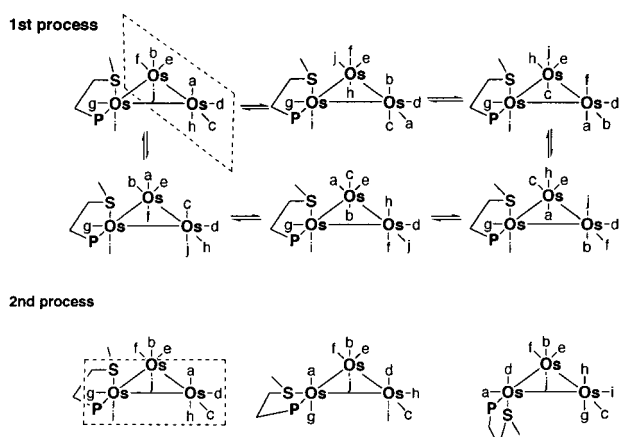


Figure 6. Variable-temperature $^{13}\text{C}\{^1\text{H}\}$ NMR spectra of 1,1-[$\text{Os}_3(\text{CO})_{10}(\text{Ph}_2\text{PCH}_2\text{CH}_2\text{SMe})$], **4**.

Scheme 2. Possible Dynamic Processes Operating in 1,1-[$\text{Os}_3(\text{CO})_{10}(\text{Ph}_2\text{PCH}_2\text{CH}_2\text{SMe})$] (4)



This process may be caused by dissociation of the thioether moiety of the P,S ligand or participation of the sulfur in the exchange (cf. Scheme 2). As in the case of **2**, the phosphine moiety is less likely to occupy an axial site due to steric and electronic preferences. As the sulfur atom is a part of the ligand, it is restricted to undergo exchange with the carbonyls labeled *g* and *i* in Figure 6; as a consequence, the carbonyl labeled *e* does not undergo exchange. All carbonyls except *g* exchange at room temperature.

The observed chemical shift at 41.55 ppm for the singlet found in the $^{31}\text{P}\{^1\text{H}\}$ spectrum of 1,1-[$\text{Os}_3(\text{CO})_{10}(\text{Ph}_2\text{PCH}_2\text{CH}_2\text{SMe})$] (**4**) is considerably higher than those observed for the compounds 1,2-[$\text{Os}_3(\text{CO})_{10}(\mu\text{-Ph}_2\text{PCH}_2\text{CH}_2\text{SMe})$] (**2**) and [$\text{Os}_3(\text{CO})_{11}(\text{Ph}_2\text{PCH}_2\text{CH}_2\text{SMe})$]

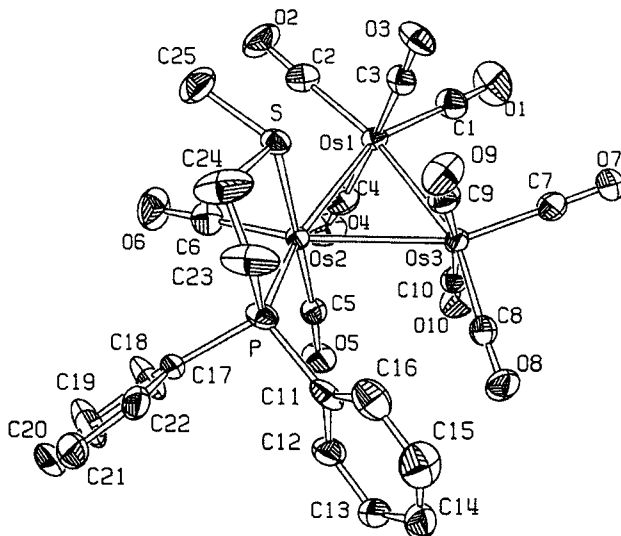


Figure 7. ORTEP drawing of S, C-1,1-[$\text{Os}_3(\text{CO})_{10}(\text{Ph}_2\text{PCH}_2\text{CH}_2\text{SMe})$], **4**. Thermal ellipsoids are drawn at the 30% level. Hydrogen atoms have been omitted for clarity.

(1). One explanation for the difference in chemical shift between **4** and **1** may be that the phosphorus atom in compound **4** is part of a five-membered ring. The size of phosphorus chemical shifts are often indicative of the ring size of chelated and bridging complexes.^{28,29} Shapley et al.³⁰ have used the change in chemical shift due to the ring effect, $\Delta\delta$ [= δ (coordinated ligand) – δ (free ligand)],²⁸ to determine the mode of bonding in the diphosphine-substituted tetranuclear cluster [$(\mu\text{-H})_4\text{Ru}_4(\text{CO})_{10}(\mu\text{-dppe})$], and Meek et al.³¹ have used similar arguments for the characterization of some five-coordinate Co(I) and Ni(II) complexes containing a tripod ligand. It is notable that the coordination chemical shifts of 1,2-[$\text{Os}_3(\text{CO})_{10}(\mu\text{-Ph}_2\text{PCH}_2\text{CH}_2\text{SMe})$] (**2**) and 1,2-[$\text{Os}_3(\text{CO})_{10}(\mu\text{-dppe})$]⁸ are very similar. The X-ray structures of 1,2-[$\text{Os}_3(\text{CO})_{10}(\mu\text{-Ph}_2\text{PCH}_2\text{CH}_2\text{SMe})$] and 1,2-[$\text{Os}_3(\text{CO})_{10}(\mu\text{-dppe})$] show that the bidentate ligands are coordinated in similar modes in these clusters. On the other hand, the chemical shift of 1,1-[$\text{Os}_3(\text{CO})_{10}(\text{Ph}_2\text{PCH}_2\text{CH}_2\text{SMe})$] (**4**) is significantly higher than for 1,1-[$\text{Os}_3(\text{CO})_{10}(\text{dppe})$]. This difference may be explained by the difference in molecular structures of the two clusters: the donor atoms are arranged in an axial-equatorial mode in **4** but in an equatorial-equatorial mode in 1,1-[$\text{Os}_3(\text{CO})_{10}(\text{dppe})$].

Crystal and Molecular Structure of 4. To confirm the structure of **4** and compare its structural parameters to those of **2**, its crystal structure was determined by X-ray diffraction. The molecular structure of **4** is depicted in Figure 7, and relevant bond lengths and angles are reported in Table 3. The coordination of the P,S ligand to one osmium through the phosphorus [Os(2)–P 2.324(3) Å], which occupies an equatorial site, and through the S atom in an axial position results in the formation of a skewed five-membered Os–P–C–C–S

(28) (a) Garrou, P. E. *Chem. Rev.* **1981**, *81*, 229. (b) Garrou, P. E. *Inorg. Chem.* **1975**, *14*, 1435.

(29) Grim, S. O.; Briggs, W. L.; Barth, R. C.; Tolman, C. A.; Jesson, J. P. *Inorg. Chem.* **1974**, *13*, 1095.

(30) Churchill, M. R.; Laszewycz, K. A.; Shapley, J. R.; Richter, S. I. *Inorg. Chem.* **1980**, *19*, 1277.

(31) Hohman, W. H.; K., D. J.; Meek, D. W. *Inorg. Chem.* **1986**, *25*, 616.

Table 3. Selected Bond Lengths (Å) and Angles (deg) for 1,1-[Os₃(CO)₁₀(Ph₂PCH₂CH₂SMe)] (4)

Os(1)–Os(2)	2.872(2)	Os(2)–C(6)	1.86(1)
Os(2)–Os(3)	2.919(2)	Os(3)–C(7)	1.90(1)
Os(1)–Os(3)	2.879(2)	Os(3)–C(8)	1.91(1)
Os(2)–P	2.324(4)	Os(3)–C(9)	1.95(2)
Os(2)–S	2.446(3)	Os(3)–C(10)	1.95(2)
S–C(25)	1.80(2)	C(1)–O(1)	1.12(2)
S–C(24)	1.80(1)	C(2)–O(2)	1.13(2)
P–C(23)	1.83(1)	C(3)–O(3)	1.15(2)
P–C(17)	1.82(1)	C(4)–O(4)	1.13(2)
P–C(11)	1.85(1)	C(5)–O(5)	1.17(2)
C(23)–C(24)	1.49(2)	C(6)–O(6)	1.19(2)
Os(1)–C(1)	1.92(1)	C(7)–O(7)	1.15(2)
Os(1)–C(2)	1.90(1)	C(8)–O(8)	1.12(2)
Os(1)–C(3)	1.94(1)	C(9)–O(9)	1.12(2)
Os(1)–C(4)	1.95(2)	C(10)–O(10)	1.14(2)
Os(2)–C(5)	1.85(1)		
S–Os(2)–P	83.7(1)	C(9)–Os(3)–Os(1)	94.8(4)
Os(2)–S–C(24)	104.1(6)	C(7)–Os(3)–C(8)	97.5(6)
S–C(24)–C(23)	114(1)	C(25)–S–C(24)	96(1)
C(24)–C(23)–P	114(2)	Os(2)–S–C(24)	104.1(6)
C(23)–P–Os(2)	107.6(5)	S–Os(2)–C(6)	89.5(4)
C(9)–Os(3)–Os(2)	78.8(4)	C(6)–Os(2)–P	100.3(5)
C(10)–Os(3)–Os(2)	94.2(4)	C(5)–Os(2)–Os(3)	79.4(4)
C(5)–Os(2)–S	174.7(4)	C(5)–Os(2)–Os(1)	97.5(4)
C(5)–Os(2)–C(6)	93.3(5)	C(3)–Os(1)–C(4)	171.5(6)
C(9)–Os(3)–Os(2)	78.8(4)		

metallacycle. The Os–S bond is longer than that in the 1,2-isomer [2.446(3) vs 2.376(3) Å], and this lengthening can be ascribed to the fact that in the 1,1-isomer the sulfur occupies an axial position and in the 1,2-isomer an equatorial one. A similar bond distance has for example been reported for the Os–S(axial) [2.449(8) Å] interaction in the cluster [Os₃(μ -H)(μ -MeSC₄H₂S)(CO)₁₀], where the 2-methylthiophene ligand bridges an Os–Os edge through the sulfur and the 3-carbon of the thiophene ring.³² The P–Os–S bite angle is 83.7(1)° and the methyl bound to the S atom is pointing toward the outer region in order not to get in close contact with the axial CO ligands. The Os–Os distances range from 2.872 to 2.919(2) Å, the longest being that *cis* to the phosphorus atom in order to relieve the steric interactions due to the ligand bulk.

A significant twisting of the Os(CO)₄ units to give a *D*₃-type conformation is observed, in contrast with the *D*_{3h} conformation of the parent [Os₃(CO)₁₂]. The axial carbonyls are also more twisted with respect to each other in 1,1-[Os₃(CO)₁₀(Ph₂PCH₂CH₂SMe)] (**4**) than in the meta-stable 1,2-isomer **2**; the degree of distortion can be measured by the C(ax)–M–M–C(ax) dihedral (torsion) angles.^{19a} For derivatives of [M₃(CO)₁₂] (M = Ru, Os), it is generally observed that these torsion angles increase on successive replacement of equatorial carbonyls with bulkier ligands.¹⁹ The average value of the torsion angles for 1,1-[Os₃(CO)₁₀(Ph₂PCH₂CH₂SMe)] (**4**) is 26.1°, while in 1,2-[Os₃(CO)₁₀(μ -Ph₂PCH₂CH₂SMe)] (**2**) it is 7.8°. The steric influence of the coordinated P,S ligand is a possible cause of the strong twisting of the axial carbonyls of **4**, but the influence of crystal packing forces cannot be excluded. There is also some twisting in the Os(CO)₂(PS) fragment, which results in the phosphorus atom being displaced from the Os₃ plane by 0.537(3) Å.

DFT calculations indicate that **4** is indeed more stable than **2**, by 23 kJ/mol. Cluster **4** is chiral as a conse-

(32) Arce, A. J.; Deeming, A. J.; De Sanctis, Y.; Speel, D. M.; Di Trapani, A. *J. Organomet. Chem.* **1999**, *580*, 370.

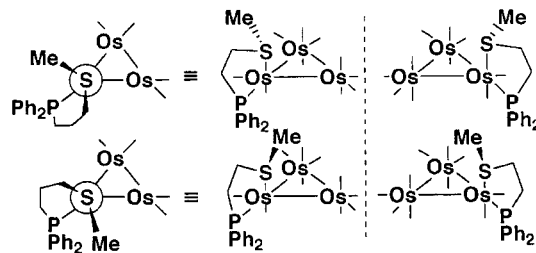


Figure 8. Possible isomers of 1,1-[Os₃(CO)₁₀(Ph₂PCH₂CH₂SMe)], **4**.

quence of coordination of the sulfur atom and the axial–equatorial coordination mode of the ligand. Two diastereomeric pairs are possible (Figure 8): the two enantiomeric pairs *S,C/R,A* and *S,A/R,C* (where *C* and *A* are IUPAC stereochemical descriptors³⁴ for the formal octahedral environment of Os2). However, in the crystal only the stereoisomer with the absolute configuration *S* at the sulfur and *C* at the Os atom is present, and the chiral conformation of the metallacycle ring is λ (cf. Figure 7). To estimate the energy difference between the two possible diastereomers, molecular mechanics calculations were made using the Merck MMFF94³⁴ force field within the Spartan 4.1 program package. The free energies of the *S,C*- and *R,C*-isomers were calculated to be -1520 and -1436 kJ/mol, respectively; that is, the energy difference between the isomers is larger than the calculated energy difference between **2** and **4**.

Studies of the Isomerization Reaction. Isomerization reactions involving conversion of bridging to chelating coordination modes of diphosphines have been observed for [H₄Ru₄(CO)₁₀(diphosphine clusters)] (diphosphine = dppe,³⁵ prophos,³⁶ bdpp³⁷). In the case of dppe³⁵ the isomerization reaction occurs under mild thermolysis, while the corresponding reactions for the other phosphines require heating at relatively high temperatures. It should be noted that all 12 ligand positions in a tetrahedral H₄Ru₄ cluster are equivalent from steric and electronic viewpoints when the positions of the hydrides are disregarded. This is not the case for triangular osmium clusters, where the axial and equatorial ligand environments are significantly different. 1,2-Bridging and 1,1-chelating isomers of triosmium clusters containing bidentate ligands have been observed previously; examples include 1,1- and 1,2-[Os₃(CO)₁₀(dppe)]. However, these isomers were prepared from different starting materials and were not found to interconvert. In addition, the 1,1-isomers have a different structure from that of **4**; that is, both phosphine moieties coordinate in equatorial positions. To our knowledge, the present isomerization reaction is the first example of a 1,2-bridging ligand, with both donors in equatorial positions, converting to a 1,1-(axial, equatorial) coordination mode. Furthermore, the apparent

(33) Leigh, G. J., Ed. *Nomenclature of Inorganic Chemistry*, IUPAC recommendations 1990; Blackwell Scientific Publications: Oxford, 1990; pp 159–189.

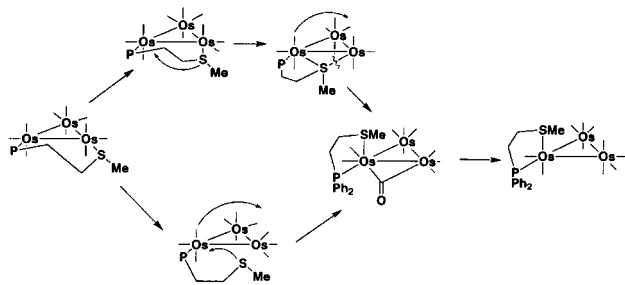
(34) (a) Halgren, T. A. *J. Comput. Chem.* **1996**, *17*, 490 (b) Halgren, T. A.; Nachbar R. B. *J. Comput. Chem.* **1996**, *17*, 587 (c) Halgren, T. A. *J. Comput. Chem.* **1996**, *17*, 616.

(35) Churchill, M. R.; Laszewycz, R. A.; Richter, S. I.; Shapley, J. R. *Inorg. Chem.* **1980**, *19*, 1277.

(36) Puga, J.; Arce, A.; Braga, D.; Centritto, N.; Grepioni, F.; Castillo, R.; Ascanio, J. *Inorg. Chem.* **1987**, *26*, 867.

(37) Homanen, P.; Persson, R.; Haukka, M.; Pakkanen, T. A.; Nordlander, E. *Organometallics* **2000**, *19*, 5568.

Scheme 3. Plausible Reaction Mechanisms for the Isomerization of **2 into **4** Involving Either (i) Dissociation of the P,S Ligand or (ii) Intramolecular Nucleophilic Attack by the Coordinated Sulfur**



low activation barrier for this isomerization is unprecedented in this kind of system.

Two plausible mechanisms for the isomerization may be envisaged (Scheme 3). In a dissociative mechanism, dissociation of the thioether moiety in **2**, followed by the transfer of one carbonyl from the $\text{Os}(\text{CO})_3(\text{P},\text{S})$ moiety to the $\text{Os}(\text{CO})_3$ fragment (via an intermediate containing a bridging carbonyl), and subsequent coordination of the sulfur at the vacant coordination site would render **4**. In an associative mechanism, a nucleophilic attack of the sulfur atom on the $\text{Os}(\text{CO})_3$ (phosphine) fragment of **2** coupled with carbonyl transfer would render **4**.

Kinetic Studies. To provide more information on the mechanism of the isomerization reaction, the kinetics of the conversion of **2** to **4** were studied by IR and NMR spectrometry. The derived rate constants for the two methods were found to be very similar when the experiments were carried out under identical conditions. Rate constants for the disappearance of **2** ($k_{\text{obs}1}$) and appearance of **4** ($k_{\text{obs}2}$) were obtained. No significant change of the observed rate constants could be observed when the initial concentration of **2** was varied between 0.73 and 24 mM. The independence of k_{obs} on the concentration of **2** is in agreement with a unimolecular reaction mechanism.

IR Spectroscopy. The isomerization reaction was monitored in dichloromethane by following the increase of the ν_{CO} absorption band at 2039 cm^{-1} due to the product **4**, the intensity of which was found to be linearly correlated to the concentration of **2** at $25\text{ }^\circ\text{C}$. The values of $k_{\text{obs}2}$ obtained by this method were similar to the corresponding rate constants obtained by measuring the reaction in CD_2Cl_2 by NMR.

NMR Spectroscopy. The reaction was studied by ^1H and $^{31}\text{P}\{^1\text{H}\}$ NMR in separate experiments at higher concentrations (8–25 mM) of **2**. Rate constants ($k_{\text{obs}1}$ and $k_{\text{obs}2}$) were derived from the time dependence of the intensities of the singlets at 2.86 ppm ($^{31}\text{P} - 1.0\text{ ppm}$) representing the reactant **2** and at 2.63 ppm ($^{31}\text{P} 38\text{ ppm}$) for the product **4**. The sums of these intensities were constant during the conversion (Figure 9), suggesting a pure conversion from **2** to **4**.

Solvent Dependence. The solvent dependence of the reaction rate at 298 K was also studied by both IR and NMR spectroscopy. The results showed that the reaction rate decreased with decreasing dielectric constant of the solvent: $k(\text{DMF}) \gg k(\text{MeCN}) > k(1,2\text{-dichloroethane}) \approx k(\text{CH}_2\text{Cl}_2) > k(\text{hexane})$. A decrease of the conversion rate by approximately 1 order of magnitude as compared to

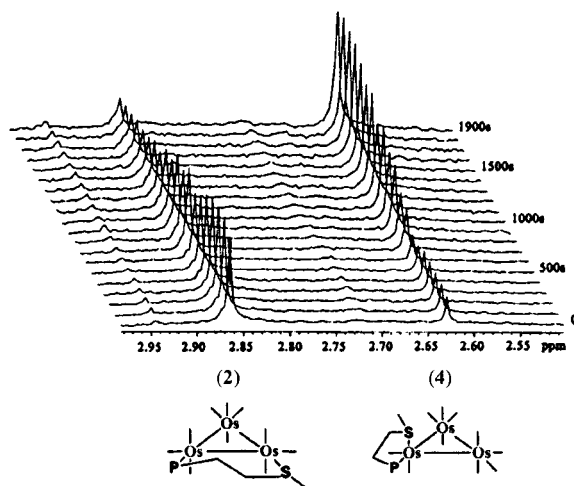


Figure 9. ^1H NMR spectra showing the conversion of **2** into **4** as monitored by the disappearance of the methyl resonance for **2** and appearance of the corresponding resonance for **4**.

the rate in 1,2-dichloroethane could be observed when *n*-hexane was used as solvent. In contrast, the conversion rate increased by a factor of approximately 4 when acetonitrile was used. The reaction was too fast to be measured by NMR when DMF was used as solvent.

To determine the activation parameters for the isomerization, the reaction was studied by ^1H NMR in the temperature range $40\text{--}65\text{ }^\circ\text{C}$ using 1,2-dichloroethane as solvent. A direct conversion of **2** to **4** permits the use of all observed rate constants to derive activation parameters, and the following parameters were calculated using the logarithmic form of the Eyring equation:

$$\ln\left(\frac{k}{T}\right) = \ln\left(\frac{\kappa k_{\text{b}} T}{hc^0}\right) + \frac{\Delta S^{\ddagger}}{R} - \frac{\Delta H^{\ddagger}}{RT}$$

$\Delta G^{\ddagger} = 97 \pm 8\text{ kJ/mol}$, $\Delta H^{\ddagger} = 79 \pm 8\text{ kJ/mol}$, $\Delta S^{\ddagger} = -60 \pm 24\text{ J/mol K}$. Because of the relatively narrow temperature range used, the relative error of ΔS^{\ddagger} is considerable. Nevertheless, the negative value of the entropy term suggests that the rate-determining step is of an associative nature. We propose that this step consists of an intramolecular nucleophilic attack of the coordinated sulfur on the osmium atom to which the phosphine moiety of the P,S ligand is coordinated (cf. Scheme 3). Such a nucleophilic attack may proceed via initial migration of the coordinated sulfur into an axial position, as detected in the variable-temperature ^{13}C NMR studies of **2** (vide supra). Concomitantly (or subsequently) a carbonyl ligand is transferred to the other osmium atom involved in the process. The strong solvent dependence of the process indicates that the isomerization proceeds via a polar intermediate/transition state, which suggests that the two migrations are not synchronous. However, concerted thioether/carbonyl migration would be favored on the basis of the EAN rule. A synchronous (concerted) process may still generate a polar intermediate/transition state, as an intramolecular nucleophilic attack of the (second) lone pair of the coordinated ligand sulfur during the isomerization reaction implies a transient buildup of positive charge on the sulfur atom.

Conclusion

The ligand $\text{Ph}_2\text{PCH}_2\text{CH}_2\text{SMe}$ coordinates to trinuclear clusters as a monodentate phosphine or a bidentate P,S ligand; in no case could coordination through only the thioether moiety of the ligand be detected. When 2 equiv of $\text{Ph}_2\text{PCH}_2\text{CH}_2\text{SMe}$ are reacted with $[\text{Os}_3(\text{CO})_{10}(\text{NCMe})_2]$, both $1,2\text{-}[\text{Os}_3(\text{CO})_{10}(\mu\text{-}\text{Ph}_2\text{PCH}_2\text{CH}_2\text{SMe})]$ (**2**) and $[\text{Os}_3(\text{CO})_{10}(\text{Ph}_2\text{PCH}_2\text{CH}_2\text{SMe})_2]$ (**3**) were formed, while only **2** could be detected when 1 equiv of the ligand was used. $1,2\text{-}[\text{Os}_3(\text{CO})_{10}(\mu\text{-}\text{Ph}_2\text{PCH}_2\text{CH}_2\text{SMe})]$ is converted into $1,1\text{-}[\text{Os}_3(\text{CO})_{10}(\text{Ph}_2\text{PCH}_2\text{CH}_2\text{SMe})]$ (**4**) in an isomerization reaction with low activation barrier; kinetic studies indicate that the isomerization occurs via an associative mechanism which is proposed to involve a nucleophilic attack on an osmium atom by the coordinated sulfur in **2**. While both concerted and nonconcerted thioether/carbonyl migration processes are possible, we favor a concerted mechanism, as it will not violate the EAN rule.

Experimental Section

General Procedures. Unless otherwise stated, purification of solvents, reactions, and manipulation of compounds were carried out under a nitrogen atmosphere with use of standard Schlenk techniques. All solvents were dried by distillation over the appropriate drying agents. The starting materials $[\text{Os}_3(\text{CO})_{12-n}(\text{NCMe})_n]$ ($n = 1, 2$)³⁸ were prepared by literature methods. All chromatographic separations and ensuing work-up were carried out in open air. Thin-layer chromatography was carried out on Merck 60 0.5 mm. Columns were packed with Merck 60 (70–230 mesh ASTM) silica gel. Infrared spectra were recorded as solutions in 0.5 mm NaCl cells on a Nicolet 20SXC FT-IR spectrometer with carbon monoxide as calibrant. Fast atom bombardment (FAB) mass spectra were obtained on a JEOL SX-102 spectrometer using 3-nitrobenzyl alcohol as matrix and CsI as calibrant. Proton and ^{31}P NMR spectra were recorded on a Varian Unity 300 MHz NMR spectrometer. The ^{13}C NMR spectra were recorded on a JEOL EX400 spectrometer operating at 100.25 MHz. Microanalyses were performed by Mikrokemi AB, Uppsala, Sweden.

Synthesis of $\text{PPh}_2\text{CH}_2\text{CH}_2\text{SMe}$. Lithium wire (306 mg, 44 mmol) was added to a stirred solution of diphenylphosphine chloride (3.7 mL, 20 mmol) in THF (100 mL). The solution was then stirred at room temperature for ca. 20 h. The deep-red mixture was transferred to a flask equipped with a dropping funnel and cooled to -40°C , and ethylene sulfide (1.18 mL, 20 mmol) in THF (10 mL) was added dropwise to the stirred mixture. The reaction mixture became transparent and was allowed to warm to room temperature over a period of 1 h. To this solution, iodomethane (1.24 mL, 20 mmol) was added dropwise during a period of ca. 5 min. After 2 h, the solvent was removed in vacuo. The crude product was obtained as a gray, semitransparent oil (5.12 g). A small fraction of the substance (500 mg) was subjected to column chromatography using a 4:3 hexane/dichloromethane mixture as eluent. Two fractions were isolated; they were, in order of increasing retention time, an unidentified colorless compound (48 mg) and $\text{Ph}_2\text{PCH}_2\text{CH}_2\text{SMe}$, (181 mg, 35%). The P,S ligand precipitated as a white solid after storage at 5°C for approximately 48 h. ^1H NMR (CDCl_3 , 300 MHz, 20 °C): δ 7.35–7.45 (m, 10H, *Ph*), 2.57 (m, 2H, *CH*₂), 2.35 (m, 2H, *CH*₂), 2.12 (s, 3H, *CH*₃). $^{31}\text{P}\{\text{H}\}$ NMR (CDCl_3 , 121 MHz, 20 °C): δ -16.7 (s, 1P). C, H, S, P Anal. (Calcd): C, 69.20 (69.21); H, 6.40 (6.58); S, 12.20 (12.31); P, 12.20 (11.9).

Synthesis of $[\text{Os}_3(\text{CO})_{11}(\text{Ph}_2\text{PCH}_2\text{CH}_2\text{SMe})]$ (1**).** In a typical reaction, the cluster $[\text{Os}_3(\text{CO})_{11}(\text{NCMe})]$ (92 mg, 0.100 mmol) and $\text{Ph}_2\text{PCH}_2\text{CH}_2\text{SMe}$ (**1**; 26 mg, 0.100 mmol) were dissolved in CH_2Cl_2 (10 mL) and stirred at room temperature for ca. 2 h. The solvent was then removed under reduced pressure at 40°C . Ensuing purification by TLC (hexane/ CH_2Cl_2 , 1:1 v/v) afforded yellow $[\text{Os}_3(\text{CO})_{11}(\text{Ph}_2\text{PCH}_2\text{CH}_2\text{SMe})]$ (**2**; 72 mg, 63%). IR (hexane): $\nu(\text{CO})$ 2107 (m), 2055 (s), 2035 (m), 2020 (vs), 2002 (w), 1990 (m), 1976 (w), 1956 (vw). ^1H NMR (CDCl_3 , 300 MHz, 20 °C): δ 7.46–7.50 (m, 10H, *Ph*); 2.89 (m, 2H, *PC*₂*H*₂), 2.29 (m, 2H, *CH*₂*S*), 2.04 (s, 3H). $^{13}\text{C}\{\text{H}\}$ NMR (CD_2Cl_2 , 213 K) 192.3 (d, 1C, $J_{\text{C}-\text{P}} = 9.1$ Hz), 184.7 (s, 1C), 183.3 (s, 1C), 175.9 (s, 1C), 175.6 (s, 1C), 172.1 (s, 1C), 171.7 (s, 1C), 169.4 (s, 1C). $^{31}\text{P}\{\text{H}\}$ NMR (CDCl_3 , 121 MHz, 293 K): -11.17 (s, 1P). FAB⁺ *m/z* 1140 (M⁺).

Synthesis of $1,2\text{-}[\text{Os}_3(\text{CO})_{10}(\mu\text{-}\text{Ph}_2\text{PCH}_2\text{CH}_2\text{SMe})]$ (2**).**

Method I. The cluster $[\text{Os}_3(\text{CO})_{10}(\text{NCMe})]$ (93 mg, 0.100 mmol) and $\text{Ph}_2\text{PCH}_2\text{CH}_2\text{SMe}$ (26 mg, 0.100 mmol) were dissolved in CH_2Cl_2 (10 mL) and stirred at room temperature for 2 min. The solution was concentrated under reduced pressure. Recrystallization of the crude product in a mixture of $\text{CH}_2\text{Cl}_2/n$ -hexane at -5°C yielded orange crystals of $1,2\text{-}[\text{Os}_3(\text{CO})_{10}(\mu\text{-}\text{Ph}_2\text{PCH}_2\text{CH}_2\text{SMe})]$, **2** (62 mg, 56%).

Method II. The oxidative reagent Me_3NO (1.36 mg, 0.0181 mmol) was added as a solid to a solution of $[\text{Os}_3(\text{CO})_{11}(\text{Ph}_2\text{PCH}_2\text{CH}_2\text{SMe})]$ (20.6 mg, 0.0181 mmol) in CH_2Cl_2 (20 mL). The reaction mixture was stirred at room temperature for approximately 2 min and then concentrated under reduced pressure. Recrystallization of the crude product in a mixture of $\text{CH}_2\text{Cl}_2/n$ -hexane yielded orange crystals of **2** (13 mg, 65%). The compound was stable as a solid and could be stored for several days at room temperature. Crystals of **2** suitable for an X-ray diffraction study were grown from a $\text{CH}_2\text{Cl}_2/n$ -hexane solution at 4°C . IR (hexane): $\nu(\text{CO})$ 2093 m, 2060 w, 2055 vw, 2029 m-w, 2011 vs, 2006 vs, 1979 w, 1957 w cm^{-1} . ^1H NMR (CDCl_3 , 300 MHz, 20 °C): 7.25–7.58 (m, 10H), 2.90 (m, 2H), 2.79 (s, 3H), 2.73 (m, 2H), 2.30 (m). $^{13}\text{C}\{\text{H}\}$ NMR (CD_2Cl_2 , 213 K): 196.3 (s, 1C), 194.5 (s, 1C), 193.5 (s, 1C), 193.2 (s, 1C), 184.0 (s, 2C), 179.0 (s, 1C), 176.9 (s, 1C), 172.5 (s, 2C). $^{31}\text{P}\{\text{H}\}$ NMR (CDCl_3 , 121 MHz, 20 °C): -0.597 (s, 1P). Anal. cf. compound **4**.

Preparation of $[\text{Os}_3(\text{CO})_{10}(\text{Ph}_2\text{PCH}_2\text{CH}_2\text{SMe})_2]$ (3**).** The cluster $[\text{Os}_3(\text{CO})_{10}(\text{NCMe})]$ (100 mg, 0.107 mmol) and $\text{Ph}_2\text{PCH}_2\text{CH}_2\text{SMe}$ (57 mg, 0.214 mmol) were dissolved in CH_2Cl_2 (20 mL) and stirred at room temperature for approximately 2 h. The solution was concentrated under reduced pressure and ensuing purification by TLC (hexane/ CH_2Cl_2 , 3:2 v/v) yielded two fractions; they were, in order of increasing elution rate, yellow $[\text{Os}_3(\text{CO})_{11}(\text{Ph}_2\text{PCH}_2\text{CH}_2\text{SMe})]$ (**1**; 61 mg, 55%) and a second crude fraction. A second purification of the crude fraction by TLC (thf/n-hexane 2:3) yielded two compounds; they were, in order of increasing elution rate, red $[\text{Os}_3(\text{CO})_{10}(\text{Ph}_2\text{PCH}_2\text{CH}_2\text{SMe})_2]$ and $1,1\text{-}[\text{Os}_3(\text{CO})_{10}(\text{Ph}_2\text{PCH}_2\text{CH}_2\text{SMe})]$ (**4**, 23 mg, 0.021 mmol 20%). Data for **3**: 37 mg, 0.027 mmol, 25%. IR (CH_2Cl_2): $\nu(\text{CO})/\text{cm}^{-1}$ 2083 m, 2026 s, 1998 vs, 1964 s(br). ^1H NMR (CDCl_3 , 300 MHz, 20 °C): 7.43–7.69 (m, 20H), 2.87–2.89 (m, 4H), 2.27–2.29 (m, 4H), 2.02 (s, 3H). $^{31}\text{P}\{\text{H}\}$ NMR (CDCl_3 , 121 MHz, 20 °C): -16.1 (s, 1P(br)), -12.8 (s, 1P(br)), -11.8 s(br), 2P). FAB MS (*m/z*): obsd 1373 calcd 1372.

Synthesis of $1,1\text{-}[\text{Os}_3(\text{CO})_{10}(\text{Ph}_2\text{PCH}_2\text{CH}_2\text{SMe})]$ (4**).**

Method I. The cluster $[\text{Os}_3(\text{CO})_{10}(\text{NCMe})]$ (93 mg, 0.100 mmol) and $\text{Ph}_2\text{PCH}_2\text{CH}_2\text{SMe}$ (**1**; 26 mg, 0.100 mmol) were dissolved in CH_2Cl_2 (10 mL) and stirred at room temperature for approximately 24 h. The solution was concentrated under reduced pressure, and ensuing purification by TLC (hexane/ CH_2Cl_2 , 3:2 v/v) yielded orange $1,1\text{-}[\text{Os}_3(\text{CO})_{10}(\text{Ph}_2\text{PCH}_2\text{CH}_2\text{SMe})]$ (**4**; 61 mg, 55%).

Method II. The oxidative reagent Me_3NO (1.36 mg, 0.0181 mmol) was added as a solid to a solution of $[\text{Os}_3(\text{CO})_{11}(\text{Ph}_2\text{PCH}_2\text{CH}_2\text{SMe})]$ (20.6 mg, 0.0181 mmol) in CH_2Cl_2 (20 mL). The reaction mixture was stirred at room temperature until

Table 4. Crystal Data and Experimental Details for $[\text{Os}_3(\text{CO})_{11}(\text{Ph}_2\text{PCH}_2\text{CH}_2\text{SMe})]$ (1), $[\text{1,2-Os}_3(\text{CO})_{10}(\mu\text{-Ph}_2\text{PCH}_2\text{CH}_2\text{SMe})]$ (2), and $[\text{1,1-Os}_3(\text{CO})_{10}(\text{Ph}_2\text{PCH}_2\text{CH}_2\text{SMe})]$ (4)

formula	$\text{C}_{26}\text{H}_{17}\text{O}_{11}\text{Os}_3\text{PS}$	$\text{C}_{25}\text{H}_{17}\text{O}_{10}\text{Os}_3\text{PS}$	$\text{C}_{25}\text{H}_{17}\text{O}_{10}\text{Os}_3\text{PS}$
<i>M</i>	1139.03	1111.02	1111.02
temperature, K	293(2)	293(2)	293(2)
wavelength, Å	0.71073	0.71073	0.71073
cryst symmetry	monoclinic	triclinic	monoclinic
space group	$P2_1/n$ (No. 14)	$P\bar{1}$ (No. 2)	$P2_1$ (No. 4)
<i>a</i> , Å	8.542(2)	11.415(7)	8.661(6)
<i>b</i> , Å	10.452(2)	11.413(3)	16.427(9)
<i>c</i> , Å	34.198(6)	11.940(5)	11.028(8)
α , deg	90	93.02(3)	90
β , deg	91.18(2)	95.65(4)	111.96(5)
γ , deg	90	111.47(4)	90
cell volume, Å ³	3053(1)	1434(1)	1455(2)
<i>Z</i>	4	2	2
D_c , Mg m ⁻³	2.478	2.573	2.536
$\mu(\text{Mo K}\alpha)$, mm ⁻¹	12.633	13.441	13.245
<i>F</i> (000)	2080	1012	1012
cryst size, mm	0.35 × 0.35 × 0.40	0.15 × 0.20 × 0.30	0.15 × 0.20 × 0.25
θ limits, deg	2–31	2–30	2–28
no. of reflns collected	7781(± <i>h</i> , + <i>k</i> , + <i>l</i>)	8296(± <i>h</i> , ± <i>k</i> , + <i>l</i>)	7317(± <i>h</i> , ± <i>k</i> , + <i>l</i>)
no. of unique obsd reflns [$F_o > 4\sigma(F_o)$]	4970	5328	6207
goodness of fit on F^2	0.957	1.027	1.055
$R_1(F)$, ^a $wR_2(F^2)$ ^b	0.0525, 0.1261	0.0526, 0.1378	0.0335, 0.0902
weighting scheme	$a = 0.0765$, $b = 0^b$	$a = 0.0889$, $b = 9.9923^b$	$a = 0.0533$, $b = 9.2526^b$
largest diff peak and hole, e Å ⁻³	1.60 and -1.68	2.08 and -2.37	1.86 and -1.95

^a $R_1 = \sum ||F_o| - |F_c||/\sum |F_o|$. ^b $wR_2 = [\sum (F_o^2 - F_c^2)^2 / \sum (F_o^2)^2]^{1/2}$ where $w = 1/[a^2(F_o^2) + (aP)^2 + bP]$ and $P = (F_o^2 + 2F_c^2)/3$.

no $\nu_{\text{C}-\text{O}}$ resonances due to **2** could be detected in the IR spectrum (approximately 24 h.) The solution was concentrated under reduced pressure, and ensuing purification by TLC (hexane/CH₂Cl₂, 3:2 v/v) yielded orange 1,1-[Os₃(CO)₁₀(Ph₂PCH₂CH₂SMe)] (**4**; 68 mg, 62%). IR (hexane): $\nu(\text{CO})$ 2088 m, 2040 s, 2011 vs, 1996 vs, 1983 mw, 1970 w, 1960 vw, 1923 w (br). ¹H NMR (CDCl₃, 300 MHz, 20 °C): 7.30–7.68 (m, 10H), 2.98 (m, 2H), 2.81 (m, 2H) 2.31 (m), 2.63 (s, 3H). ¹³C{¹H} NMR (CD₂Cl₂, 205 K): 190.0 (t, ²J_{C-C} = 33 Hz, 1C); 189.7 (d, ²J_{C-P} = 9.1 Hz, 1C); 186.6 (t, ²J_{C-C} = 33 Hz, 1C); 186.4 (t, ²J_{C-C} = 33 Hz, 1C); 185.1 (t, ²J_{C-C} = 33 Hz, 1C); 181.2 (s, 1C); 177.4 (s, 1C); 176.7 (s, 1C); 173.6 (s, 1C); 172.3 (s, 1C). ³¹P{¹H} NMR (CDCl₃, 121 MHz, 20 °C): 41.55 (s, 1P). Anal. (Calcd): C, 27.50 (27.65); H, 1.74 (1.70); S, 2.60 (2.85); P, 2.80 (2.76).

Kinetics of the Conversion of 1,2-[Os₃(CO)₁₀(μ -Ph₂PCH₂CH₂SMe)] (2**) into 1,1-[Os₃(CO)₁₀(Ph₂PCH₂CH₂SMe)] (**4**).** **Kinetics Measured by ¹H NMR.** Cluster **2** was generated in situ in the following way: the ligand (6.80 mg, 0.0261 mmol) was dissolved in 700 μ L of CD₂Cl₂ in a NMR tube at room temperature. The cluster [Os₃(CO)₁₀(NCMe)₂] (22.84 mg, 0.02449 mmol) was added to the solution, and the solution was shaken until all solids were dissolved. The NMR tube was then inserted into the spectrometer, and the experiment was started.

Temperature-Controlled Experiments. A stock 42.75 mM solution of 1,2-[Os₃(CO)₁₀(μ -Ph₂PCH₂CH₂SMe)] (**2**) was prepared by dissolving **2** (94 mg) in dichloromethane (2.00 mL). The solvent was precooled in a freezer (-20 °C) before addition of **2** in order to prevent formation of **4**. This solution could be stored at -20 °C for a week or longer. The purity of the stock solution was checked by IR before every experiment. In each experiment, a volume corresponding to 10 mg of **2** was transferred to a glass vial via micropipet. The solution was dried under a nitrogen stream and was stored over dry ice until the start of the experiment, when it was redissolved in 500 μ L of solvent. The solution was transferred to a NMR tube, and the tube was rapidly inserted into the spectrometer. The temperature of the probe was controlled and kept stable at the decided temperature for at least 15 min prior to initiation of the experiments.

Measurement of the Kinetics. In all experiments, the solutions were periodically analyzed by using a preacquisition delay sequence. A total number of 30 arrayed spectra was collected in each experiment. The absolute values of intensities

(peak heights and areas) of the resonances were measured. The change of intensity of each resonance was plotted vs time. The obtained data were then curve fitted by least-squares refinement using KaleidaGraph v.3.0.4.

Kinetics Measured by IR Spectroscopy. The concentration of **4** (0.041–1.31 mM of **4** in dichloromethane) could be linearly correlated to the intensity of the ν_{CO} absorption band at 2039 cm⁻¹ measured in absorbance mode. In one of the experiments, cluster **2** was generated in situ by mixing Ph₂PCH₂CH₂SMe (16.30 mg, 17.48 μ mol) and the cluster [Os₃(CO)₁₀(NCMe)₂] (16.30 mg, 17.48 μ mol) in 22 mL of dichloromethane at room temperature. A total number of 30 IR spectra were recorded periodically during a period of 130 h.

Temperature-Controlled Experiments. Cluster **2** (1–2 mg) was dissolved in 5.00 mL of the decided solvent and transferred to a Schlenk tube. The tube was immediately placed in temperature-controlling equipment that was stable at the actual temperature for at least 30 min before starting the experiments. The solution was then periodically analyzed by transferring small amounts of the solution to an IR cell. All spectra were recorded at room temperature. A negligible conversion of **2** to **4** upon warming to room temperature was assumed. The increase of intensity of the absorption peak at $\nu_{\text{CO}} = 2039$ cm⁻¹ was measured in absorbance mode and plotted vs time. As in the case of the NMR data, the obtained IR data were curve fitted by least-squares refinement.

X-ray Structure Determination of [Os₃(CO)₁₁(Ph₂PCH₂CH₂SMe)], 1,1-[Os₃(CO)₁₀(Ph₂PCH₂CH₂SMe)], and 1,2-[Os₃(CO)₁₀(μ -Ph₂PCH₂CH₂SMe)]. All X-ray diffraction experiments were carried out at room temperature on a fully automated CAD4 diffractometer. The unit cell parameters were determined from 25 randomly selected reflections by using automatic search, indexing, and least-squares routines. Crystal data and details of the data collections are given in Table 4. Intensity data were corrected for Lorentz and polarization effects. Empirical absorption corrections were applied by using the azimuthal scan method.³⁹ The metal atom positions were determined by direct methods using SIR97⁴⁰

(39) North, A. C. T.; Phillips, D. C.; Mathews, F. S. *Acta Crystallogr.* **1968**, *A24*, 351.

(40) Altomare, A.; Burla, M. C.; Camalli, M.; Cascarano, G. L.; Giacovazzo, C.; Guagliardi, A.; Molteri, A. G. G.; Polidori, G.; Spagna, R. *SIR97: a new tool for crystal structure determination and refinement*. *J. Appl. Crystallogr.* **1999**, *32*, 115.

for $[\text{Os}_3(\text{CO})_{11}(\text{Ph}_2\text{PCH}_2\text{CH}_2\text{SMe})]$ (**1**) and SHELXS 86⁴¹ for 1,2- $[\text{Os}_3(\text{CO})_{10}(\text{Ph}_2\text{PCH}_2\text{CH}_2\text{SMe})]$ (**2**) and 1,1- $[\text{Os}_3(\text{CO})_{10}(\text{Ph}_2\text{PCH}_2\text{CH}_2\text{SMe})]$ (**4**). Least-squares refinement and difference Fourier syntheses revealed all remaining non-H atoms. The methylene and phenyl hydrogen atoms were included in idealized positions. The final refinement on F^2 proceeded by full-matrix least-squares calculations (SHELXL 93)⁴² using anisotropic thermal parameters for all the non-hydrogen atoms. The methyl, methylene, and phenyl hydrogen atoms were assigned an isotropic thermal parameter 1.5, 1.3, and 1.2 times, respectively, that of the corresponding carbon atoms. For compound **4** the absolute configuration was determined [Flack parameter 0.09(2)].

Density Functional Theory Calculations. All density functional theory calculations were performed using the Amsterdam Density Functional program package (ADF).^{43,44} The local spin density (LSD) exchange correlation potential was used with the Local Density Approximation of the correlation energy (Vosko–Wilk–Nusair).⁴⁵ Furthermore, Becke's nonlocal corrections⁴⁶ to the exchange energy and Perdew's nonlocal corrections⁴⁷ to the correlation energy were included in the calculation of the gradients.⁴⁸ The relativistic effects were

treated by a quasi-relativistic method where Darwin and mass-velocity terms are incorporated.⁴⁹ The inner shells of Os (1s–5p) were frozen. A triple- ζ STO basis set was used for the valence part of Os (5d–6s), additionally augmented by one diffuse 6p function. For C and N, the 2s and 2p valence shells were described by a triple- ζ STO basis, augmented by one 3d polarization function. For O and H a double- ζ STO basis was used. The 2s and 2p shells of C are triply split and augmented by two polarization functions (3d+4f). The models were built from the X-ray structures described above for clusters **2** and **4** with the methyl and phenyl groups being replaced by hydrogens.

Acknowledgment. This research has been sponsored by grants from the Swedish Engineering Research Council (TFR) to E.N., MURST (COFIN 2000) (to M.M. and R.G.), the University of Bologna ('Funds for Selected Research Topics', to M.M.), and the European Union TMR network *Metal Clusters in Catalysis and Organic Synthesis* (to E.N., S.A., and M.J.C.). We thank Dr. Sofi Elmrøth and Prof. Sergey Tunik for valuable discussions.

Supporting Information Available: Listings of atomic coordinates, bond lengths and angles, anisotropic thermal parameters, and hydrogen atom coordinates for $[\text{Os}_3(\text{CO})_{11}(\text{Ph}_2\text{PCH}_2\text{CH}_2\text{SMe})]$ (**1**), 1,1- $[\text{Os}_3(\text{CO})_{10}(\text{Ph}_2\text{PCH}_2\text{CH}_2\text{SMe})]$ (**2**), and 1,2- $[\text{Os}_3(\text{CO})_{10}(\text{Ph}_2\text{PCH}_2\text{CH}_2\text{SMe})]$ (**4**); observed rate constants for the kinetic measurements; calculated energies for different conformations of **2** and **4**; observed and calculated mass spectra for **1**, **3**, and **2/4**. This material is available free of charge via the Internet at <http://pubs.acs.org>.

OM010223D

(41) Sheldrick, G. M. *SHELXS 86*, Program for Crystal Structure Determination. *Acta Crystallogr.* **1990**, *A46*, 467.
 (42) Sheldrick, G. M. *SHELXL 93*, Program for crystal structure refinement; University of Göttingen, 1993.
 (43) *Amsterdam Density Functional (ADF) program*, release 2.3; Vrije Universiteit: Amsterdam, The Netherlands, 1995.

(44) (a) Baerends, E. J.; Ellis, D.; Ros, P. *Chem. Phys.* **1973**, *2*, 41. (b) Baerends, E. J.; Ros, P. *Int. J. Quantum Chem.* **1978**, *S12*, 169. (c) Boerrigter, P. M.; te Velde, G.; Baerends, E. J. *Int. J. Quantum Chem.* **1988**, *33*, 87. (d) te Velde, G.; Baerends, E. J. *J. Comput. Phys.* **1992**, *99*, 84.
 (45) Vosko, S. H.; Wilk, L.; Nusair, M. *Can. J. Phys.* **1980**, *58*, 1200.
 (46) (a) Becke, A. D. *J. Chem. Phys.* **1987**, *88*, 1053. (b) Becke, A. D. *Phys. Rev.* **1988**, *A38*, 3098.
 (47) (a) Perdew, J. P. *Phys. Rev.* **1986**, *B33*, 8822. (b) Perdew, J. P. *Phys. Rev.* **1986**, *B34*, 7406.
 (48) (a) Versluis, L.; Ziegler, T. *J. Chem. Phys.* **1988**, *88*, 322. (b) Fan, L.; Ziegler, T. *J. Chem. Phys.* **1991**, *95*, 7401.